Received: 3 May 2021 | Revised: 18 September 2021 | Accepted: 19 October 2021

DOI: 10.1111/odi.14156

ORIGINAL ARTICLE

ORAL DISEASES Leading in Oral, Maxillofacial, Head & Neck Medicine WILEY

Long non-coding RNA MRPL23-AS1 suppresses anoikis in salivary adenoid cystic carcinoma in vitro

Yin-Ran Li[1,2] | Min Fu[1,2] | Ye-Qing Song[1] | Sheng-Lin Li[1,2] | Xi-Yuan Ge[1,2]

[1]Central Laboratory, Peking University School and Hospital of Stomatology & National Center of Stomatology & National Clinical Research Center for Oral Diseases, National Engineering Research Center of Oral Biomaterials and Digital Medical Devices & Beijing Key Laboratory of Digital Stomatology, Research Center of Engineering and Technology for Computerized Dentistry Ministry of Health & NMPA Key Laboratory for Dental Material, Beijing, China

[2]Department of Oral and Maxillofacial Surgery, Peking University School and Hospital of Stomatology, Beijing, China

Correspondence
Xi-Yuan Ge, Center Laboratory, Peking University School and Hospital of Stomatology, No.22, Zhongguancun South Avenue, Haidian District, Beijing, 100081, PR China, E-mail address: gexiyuan@bjmu.edu.cn

Abstract

Distant lung metastasis is the main factor that affects the survival rate of patients with salivary adenoid cystic carcinoma (SACC). Anoikis resistance is a feature of tumor cells that easily metastasize. The long non-coding RNA (lncRNA) MRPL23 antisense RNA 1 (MPRL23-AS1) is related to lung metastasis in SACC, but its role in anoikis resistance is unknown. After altering MPRL23-AS1 expression in SACC cells, anoikis resistance was detected by calcein AM/PI staining and annexin V/PI flow cytometry. The apoptosis marker activated caspase-3 and the bcl-2/bax ratio were detected by Western blotting. The relationship between MPRL23-AS1 and the promoter of the potential downstream target gene p19INK4D was identified by chromatin immunoprecipitation (ChIP)-PCR assay. p19INK4D expression in patient tissues was determined using qRT-PCR and immunohistochemistry. The functional experiments showed that MPRL23-AS1 could promote anoikis resistance in vitro. MRPL23-AS1 recruited the EZH2 to the promoter region of p19INK4D, inhibited p19INK4D expression, and promoted tumor cell anoikis resistance. p19INK4D overexpression did not affect anoikis in attached cells; however, it attenuated the anoikis resistance effect of MPRL23-AS1 in suspension cells. p19INK4D expression was significantly lower in SACC tissues than in normal tissues. The novel MRPL23-AS1/p19INK4D axis may be a potential SACC biomarker or therapeutic target.

KEYWORDS
anoikis, LncRNA, MRPL23-AS1, p19INK4D, salivary adenoid cystic carcinoma

1 | INTRODUCTION

Adenoid cystic carcinoma (ACC) is an uncommon malignant tumor that arises within secretory glands, mainly the salivary glands, and accounts for approximately 25% of major salivary gland malignancies and 50% of minor salivary gland malignancies (Chen et al., 2012; Ellington et al., 2012; Tincani et al., 2006). Salivary ACC (SACC) is typically characterized by slow growth and is prone to nerve invasion in the early stage and pulmonary metastasis, the incidence of which is up to 47.8%, in the late stage (Kokemueller et al., 2004; Rapidis et al., 2005). Late-onset distant metastasis is the most common factor related to the poor prognosis of SACC (Gao et al., 2013). The 10-year overall survival rate of SACC is approximately 50%, but local recurrence and distant recurrence are often observed after a short disease-free interval (Spiro & Huvos, 1992; Terhaard et al., 2004). After the occurrence of metastasis, the median survival time of ACC is approximately 3 years (Spiro & Huvos, 1992; van der Wal et al., 2002), and rapid disease progression after metastasis leads to death within two years in one-third of patients (Spiro, 1997). Although tumor metastasis is one of the main causes of SACC-related death, its mechanism of action remains unclear (Coca-Pelaz et al., 2015). At present, radical surgical resection and adjuvant postoperative radiotherapy are conducive to controlling the primary lesions, but the overall prognosis of SACC patients is poor, and the long-term outcomes are unsatisfactory (Lloyd et al., 2011). Therefore, it is imperative to

clarify the biological molecular mechanism of SACC lung metastasis to improve clinical outcomes.

Anoikis regulation is a key step in cancer metastasis. Metastasis is defined as a multifaceted event that enhances the spread of tumor cells from the primary tumor to the blood vessels and lymphatic system and ultimately results in the proliferation of tumor cells in different parts of the body (Chen et al., 2020; Kong et al., 2019; Yao et al., 2018). Tumor metastasis has several steps, including epithelial to mesenchymal transition (EMT), migration through the circulatory system, and finally the formation of metastatic lesions in the host organ (Gillies et al., 2008). One of main obstacles to metastasis is a type of apoptosis called anoikis, which starts with the separation of cells from the natural extracellular matrix and prevents the separated cells from attaching to other body organs. Tumor cells need to acquire different characteristics, including enhanced invasiveness and resistance to anoikis, to form tumor sites in distant parts of the body (Tajbakhsh et al., 2019).

Long non-coding RNAs (lncRNAs), a class of transcripts >200 nucleotides (nts) in length, exhibit poor protein-coding potential. LncRNAs play complex and extensive roles in the development and progression of various cancers (Kapranov et al., 2007; Wang & Chang, 2011). Previous studies have reported that lncRNAs, such as the oncogenes lncRNA HOTAIR (Topel et al., 2020) and lncRNA VAL (Tian et al., 2020) and the tumor suppressor MAPK8IP1P2 (Liu et al., 2020), can affect anoikis progression. Therefore, lncRNAs affecting anoikis resistance in cancer have been investigated in numerous studies, but their function remains controversial. MRPL23 antisense RNA 1 (MRPL23-AS1) has been examined in several studies. The overexpression of MRPL23-AS1 is related to a higher metastatic potential (Chen et al., 2020) and a higher risk of poor overall survival (Zhang et al., 2021). Our previous research showed that MRPL23-AS1 promotes SACC cell EMT and lung metastasis (Chen et al., 2020). Furthermore, to our knowledge, the roles of MRPL23-AS1 in the progression of anoikis and its downstream molecules in SACC have not been previously reported.

p19INK4D is an inhibitor of cyclin-dependent kinase (INK4) family members, which include the p15INK4B, p16INK4A, and p18INK4C proteins (Cheng, 2004). The cyclin-dependent kinase inhibitor (CDKI) family contains the INK4 family and the CIP/KIP family, which target CDK4/6 and CDK2, respectively (Besson et al., 2008; Roskoski, 2019). CDKIs inhibit the formation of the cyclin-CDK complex through competitively binding CDK, leading to arrest in the G1 phase (Spiro, 1997). p19INK4D participates in a series of physiological activities and the pathogenesis of diseases, including the cell cycle, apoptosis, DNA damage repair, cell differentiation of hematopoietic cells, and cellular senescence (Carcagno et al., 2012; Dreidax et al., 2014; Gilles et al., 2008; Hilpert et al., 2014; Sonzogni et al., 2014). Previous studies have suggested that p19INK4D promotes the apoptosis processes of several tumor cells, including malignant glioma cells (Komata et al., 2003), ER-negative breast cancer cells (Guo et al., 2013), and hepatocellular carcinoma cells (Zhou et al., 2018). The influence of p19INK4D in anoikis is unknown.

Here, we uncovered that MRPL23-AS1 negatively regulates p19INK4D expression to facilitate resistance to anoikis in SACC.

2 | MATERIALS AND METHODS

2.1 | Cell lines

The SACC-83 cell line originated from tissue isolated from a patient with SACC in 1983 (Li, 1990). The SACC-LM cell line has enhanced lung metastatic features and was generated following the injection of SACC-83 cells into the tail vein of immunodeficient mice (Dong et al., 2011; Fu et al., 2020). The SACC-83 and SACC-LM cell lines were established by the author SLL and kept at Peking University School and Hospital of Stomatology. SACC-83 and SACC-LM cells were cultivated in RPMI-1640 medium supplemented with 10% FBS (both from Gibco; Thermo Fisher Scientific, Inc.).

2.2 | Overexpression and small interfering RNA (siRNA) transfection

SACC-LM cells were transiently transfected with targeted siRNA or scrambled negative control siRNA (siNC). All individual siRNAs were designed and synthesized by RiboBio. The cells were grown in six-well plates to 30–50% confluence and transfected using riboFECTTM CP (RiboBio) according to the manufacturer's instructions. The cells were harvested after a forty-eight-hour transfection period. To overexpress MRPL23-AS1, the plasmid pcDNA-MRPL23-AS1 was constructed by introducing an EcoRI/NotI fragment containing an MRPL23-AS1 cDNA sequence into the same sites in pcDNA3.1(+). MRPL23-AS1 or pcDNA3.1(+) was transfected into SACC-83 cells using Lipofectamine 2000 (Invitrogen). To overexpress p19INK4D, the plasmid p19INK4D was constructed by introducing an EcoRI/NotI fragment containing a p19INK4D cDNA sequence into the same sites in GV492. The p19INK4D or GV492 plasmid was transfected into SACC-LM cells using Lipofectamine 2000 (Invitrogen).

2.3 | Apoptosis and cell cycle analysis with flow cytometry

To quantify live and dead cells, cells were costained with calcein acetoxymethyl (AM) and propidium iodide (PI). Briefly, the cells were collected, washed with phosphate-buffered saline (PBS), and incubated in a PBS solution containing 2 μM calcein AM and 4 μM PI in the dark for 20 min at room temperature. After washing, the cells were resuspended in PBS and imaged using a fluorescence confocal microscope (FV1000; Olympus, Tokyo, Japan).

For the apoptosis assay, costaining was performed using an annexin V-fluorescein isothiocyanate (FITC)/PI apoptosis detection kit (Keygen Biotechnology, Nanjing, China). The cells were harvested by trypsinization and resuspension and then washed with PBS. The

cells were resuspended in 300 μl of binding buffer with annexin V-FITC and PI (3 μl) and incubated in the dark at room temperature for 15 min. Binding buffer (400 μl) was then added, and the cells were analyzed using a FACScan flow cytometer (BD Biosciences, Franklin Lakes, NJ, USA).

2.4 | *qRT-PCR*

Quantification of mRNA expression was performed using FastStart Universal SYBR Green Master (ROX) reagent (Roche, USA) on an ABI 7500 Sequence Detection System. The mRNA expression of genes of interest was normalized to that of GAPDH, and the results are presented as the fold change using the ΔΔCt method with the control set as one. The primer sequences are shown in Table S1.

2.5 | Western blot analysis

Western blot assays were performed according to a standard protocol. Briefly, 40 μg of protein from cells or exosomes was separated on an SDS-PAGE gel and transferred to polyvinylidene difluoride membranes. After the membranes were blocked, primary antibodies targeting the following were used: p19INK4D (rabbit; Proteintech, China); Bax (rabbit; ABclonal, China); Bcl-2 (rabbit; ABclonal, China); and cleaved caspase-3 (rabbit; ABclonal, China). Equal protein loading was determined using anti-GAPDH (ZSGB-Bio, China) for total protein lysates. The bands were quantified using the Gel-Pro Analyzer.

2.6 | Chromatin immunoprecipitation (ChIP)

ChIP was performed using a ChIP assay kit (Beyotime) according to the manufacturer's protocol. Briefly, cross-linked chromatin was sonicated into 200–1,000-bp fragments. Chromatin was immunoprecipitated using anti-EZH2 (ab191250, Abcam) and anti-H3K27me3 (9733S, CST) antibodies. Normal human IgG (ab37415, Abcam) was used as an isotype control. The immunoprecipitated chromatin was purified and analyzed by qPCR. The primers used are listed in Table S1.

2.7 | Human tissue samples and immunohistochemical analysis

The 59 human SACC tissues (paraffin-embedded tissues) and 17 paired healthy submandibular gland (SMG) tissues (paraffin-embedded tissues) (age, 35–68 years; female:male = 10:7) used for the immunohistochemical analysis were collected from patients who received radical tumor resection at Peking University Hospital of Stomatology (Beijing, China) between 2008.08 and 2017.04. The obtained 106 human SACC specimens (frozen tissues) (age, 30–76 years; female:male = 60:46) and 26 separate healthy SMG tissues (frozen tissues) used to analyze MRPL23-AS1 and p19INK4D expression were collected between 2015.08 and 2019.07 at the Peking University School and Hospital of Stomatology. Patients had not undergone chemotherapy or radiation therapy, and the study was approved and followed the guidelines of the Ethics Committee of Peking University School and Hospital of Stomatology (permit no. PKUSSIRB-201522040). According to the relative gene expression of p19INK4D in 106 patients with SACC examined by reverse transcription-quantitative PCR (RT-qPCR), the 106 patients were classified into the high or low p19INK4D-expression group depending on the median p19INK4D relative gene expression. When the p19INK4D expression level of SACC tissue was lower than the median p19INK4D expression, the SACC tissue was classified into the low p19INK4D group; otherwise, the SACC tissue was classified into the high p19INK4D group.

Immunohistochemistry (IHC) was performed according to a standard protocol. After deparaffinization and rehydration, tissue sections were incubated in EDTA pH=8.0 buffer and heated for antigen retrieval. p19INK4D (rabbit, Proteintech, China) was applied to tissue sections overnight at 4°C. All sections were then incubated with secondary antibody for 30 min at room temperature. The immunoreactions were visualized and scored by two investigators blinded to the relative clinical outcome. The percentage of positively stained tumor cells was assessed as follows: 1 (0–10%); 2 (11–50%); 3 (51–80%); and 4 (≥81%). The staining intensity was graded as follows: 0 (no staining); 1 (weak staining); 2 (moderate staining); and 3 (strong staining). The final score was determined by the ratio of positively stained tumor cells ×staining intensity to produce scores of 0, 1, 2, 3, 4, 6, 8, 9, and 12. The IHC score ranged from 0 to 12 points: A score of 0–2 was defined as negative expression, and a score of 2–12 was defined as positive expression.

2.8 | Statistical analyses

The results were analyzed using SPSS Version 21.0 (IBM). Student's *t* tests were used to compare two groups. All numerical data represent the mean ± standard deviation (SD) from at least 3 independent experiments, unless otherwise noted. The correlation coefficients between p19INK4D expression and clinicopathological features were calculated using the chi-square test. In cases of multigroup testing, one-way analysis of variance (ANOVA) was used. A two-tailed $p < 0.05$ was considered significant.

3 | RESULTS

3.1 | *LncRNA MRPL23-AS1 promotes anoikis resistance in suspended SACC cells*

The fate of tumor cells in the circulation relies largely on their resistance to anoikis, apoptosis, and necrosis. To study the mechanisms and effects of MRPL23-AS1 on tumor cells, we prevented cell

adhesion by cultivating SACC cells on non-adherent plates to mimic the environment of cancer cells. To determine whether MRPL23-AS1 protects SACC cells from anoikis, we overexpressed MRPL23-AS1 in SACC-83 cells (Figure 1a), followed by suspension cultivation of the cells for 12 h/24 h. Calcein AM/PI costaining and flow cytometry were used to assess apoptosis. Calcein AM/PI costaining showed the number of PI-positive cells (representing those that underwent anoikis) was significantly decreased in the MRPL23-AS1-overexpression groups compared with the control groups (Figure 1b,c). Moreover, double staining with PI and annexin V-FITC by flow cytometry revealed a remarkable cell protective effect in the MRPL23-AS1-overexpression groups (Figure 1d). Subsequently,

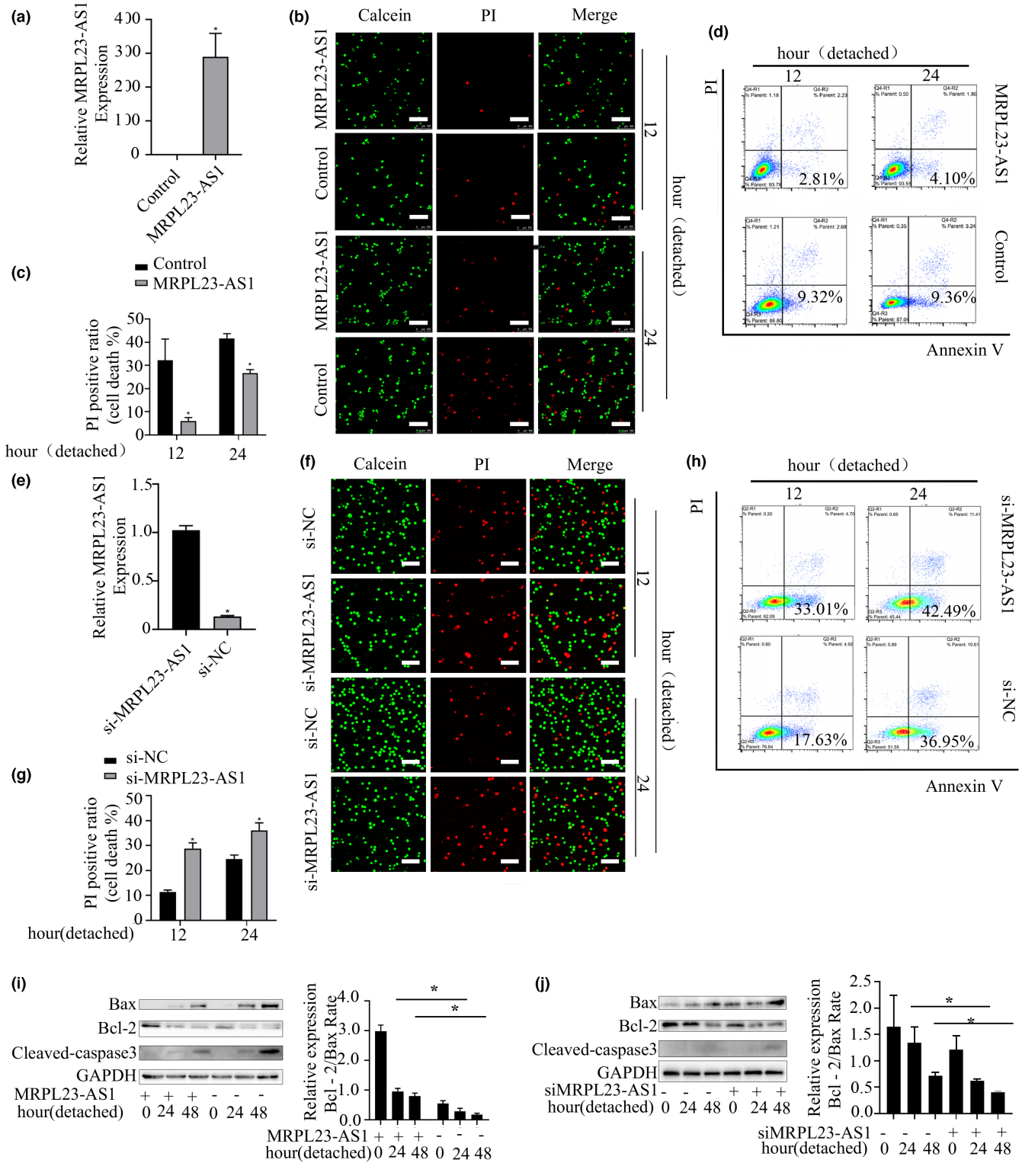

FIGURE 1 Figure Legent on next page

FIGURE 1 LncRNA MRPL23-AS1 promotes anoikis resistance in suspended SACC cells. (a) The efficiency of MRPL23-AS1 overexpression in SACC-83 cells was detected by RT-qPCR. (b-c) Calcein AM/PI staining in SACC-83 cells after MRPL23-AS1 overexpression and suspension culture for 12 and 24 h. Five fields were chosen for each group, and the cell death rate was determined. Scale bar = 100 μm. (d) After MRPL23-AS1 overexpression in SACC-83 cells and suspension culture for 12 and 24 h, annexin V-FITC-PI staining and flow cytometry were used to determine the percentage of apoptotic cells. FITC: fluorescein isothiocyanate; PI: propidium iodide. (e) The MRPL23-AS1 knockdown efficiency in SACC-LM cells was detected by RT-qPCR. (f, g) Calcein AM/PI staining in SACC-LM cells after the knockdown of MRPL23-AS1 and suspension culture for 12 and 24 h. Five fields of view were chosen, and the cell death rate was determined. Scale bar = 100 μm. (h) After the knockdown of MRPL23-AS1 in SACC-83 cells and suspension culture for 12 and 24 h, annexin V-FITC/PI staining and flow cytometry were used to determine the percentage of apoptotic cells. FITC: fluorescein isothiocyanate; PI: propidium iodide. (i) Western blot analysis of apoptosis-related protein expression after suspension culture of SACC-83 cells overexpressing MRPL23-AS1 or control vector for 24 and 48 h (left). Semiquantitative analysis of the relative expression rate of Bcl-2 and Bax (right). (j) MRPL23-AS1 was knocked down in SACC-LM cells, and after suspension culture for 24 and 48 h, Western blot analysis of apoptosis-related protein expression (left) was performed. Semiquantitative analysis of the relative expression rates of Bcl-2 and Bax (right) (*$p<0.05$; the data are expressed as the mean ± SD; $n = 3$)

MRPL23-AS1 expression was knocked down with siRNA to verify its anoikis effects in SACC-LM cells (Figure 1e). The calcein AM/PI costaining assay indicated a significantly higher death rate among cells in the MRPL23-AS1-knockdown group than in the siNC group (Figure 1f,g). To further verify whether anoikis was influenced by MRPL23-AS1, we assessed the proportion of apoptotic cells using a flow cytometry assay. The percentage of dead cells was higher in the MRPL23-AS1-knockdown group than in the siNC group (Figure 1h). Studies have shown that the death receptor pathway, activated by caspase-3, partly mediates anoikis in malignant cancer cell lines (Medema et al., 1997). To dissect the mechanism of MRPL23-AS1 in anoikis, we detected the expression of the typical apoptosis molecule caspase-3. Western blotting showed that cleaved caspase-3 expression was enhanced after MRPL23-AS1 overexpression (Figure 1i). In addition, the Bcl-2 family plays an essential role in the regulation of apoptosis (Martinou & Youle, 2011). To confirm whether this family is involved in MRPL23-AS1-induced anoikis resistance, Western blot analysis revealed a significant change in the Bcl-2/Bax expression ratio. After the overexpression of MRPL23-AS1 and suspension culture for 48 h, Western blot analysis revealed that the upregulation of the Bcl-2/Bax expression ratio was attenuated compared with that in the control groups. Overexpression of MRPL23-AS1 inhibited the decrease in the Bcl-2/Bax ratio caused by suspension culture (Figure 1i), while knockdown of MRPL23-AS1 in SACC-LM cells led to the opposite results (Figure 1j). These results indicated that the overexpression of MRPL23-AS1 in tumor cells can significantly promote anoikis resistance in tumor cells.

3.2 | *p19INK4D expression is involved in the progression of lncRNA MRPL23-AS1-induced anoikis resistance*

Our previous research showed that MRPL23-AS1 recruits the enhancer of zeste homolog 2 (EZH2) to the promoter of E-cad and promotes EMT and lung metastasis (Chen et al., 2020). We speculated that MRPL23-AS1 also performed through similar functions during the process of anoikis resistance. To identify the downstream molecules of MRPL23-AS1, a gene expression analysis was performed to identify differentially regulated genes in EZH2-silenced EMT cells. Microarray data (Joyce et al., 2009) for Caco-H2 cells are available, and a group of selected several genes (Ferraro et al., 2013) was primarily analyzed in this cell system. A subset of several genes was analyzed in SACC cells with or without suspension culture and MRPL23-AS1 (data not shown). We found that when MRPL23-AS1 expression changed during suspension culture, only p19INK4D changed accordingly. The overexpression of MRPL23-AS1 resulted in a decrease in p19INK4D in suspended tumor cells at the mRNA and protein levels (Figure 2a). In addition, the mRNA and protein levels of p19INK4D increased after the knockdown of MRPL23-AS1 (Figure 2b). However, p19INK4D expression did not change at the mRNA or protein level with or without MRPL23-AS1 (Figure 2a,b). The INK4 family of CDKIs, including p16INK4A, p15INK4B, p18INK4C, and p19INK4D, not only arrests cell cycle progression but also contributes to the apoptotic machinery. Previous studies have reported that p16INK4A negatively regulates apoptosis (Ivanchuk et al., 2001), and p16INK4A was shown to increase the anoikis resistance of tumor cells in a pancreatic carcinoma model by downregulating galectin-3, an endogenous competitor of the pro-anoikis effector galectin-1 (Sanchez-Ruderisch et al., 2010). Galectin-3 also increases caspase-3 protein expression (Diao et al., 2018). However, the relationship between MRPL23-AS1 and p19INK4D and the effect of p19INK4D on anoikis resistance are unknown. Therefore, we suspect that p19INK4D, as a homolog of p16INK4A, might act as a downstream molecule of MRPL23-AS1 in anoikis resistance processes by inhibiting caspase-3 activation. Our previous study identified that lncRNA MRPL23-AS1 could mediate the transcriptional silencing of E-cadherin by forming an RNA-protein complex with EZH2 (Chen et al., 2020). We hypothesize that MRPL23-AS1 has a similar regulatory effect on p19INK4D. To test our hypothesis of the molecular mechanism of MRPL23-AS1 induction in SACC cells, we applied the Animal TFDB database (http://bioinfo.life.hust.edu.cn/AnimalTFDB/) (Hu et al., 2019) to predict the protein binding site in the p19INK4D promoter region (Figure 2c). Next, we designed three pairs of primers for the p19INK4D promoter region based on the predicted binding site. A ChIP-qPCR assay was used to verify the binding protein (Figure 2c). Then, ChIP-qPCR assays showed that H3K27me3 and EZH2 pulled down more p19INK4D promoter sequences than did IgG (Figure 2d). MRPL23-AS1 overexpression in suspended SACC-83 cells increased the binding of H3K27me3 and EZH2 to the p19INK4D promoter region compared with that in the control groups (Figure 2e). These results suggest that when an anoikis stimulus was applied, the binding of EZH2 to the promoter was affected and reduced, while MRPL23-AS1 promoted the binding of EZH2 to the promoter. In addition, a significant negative correlation between

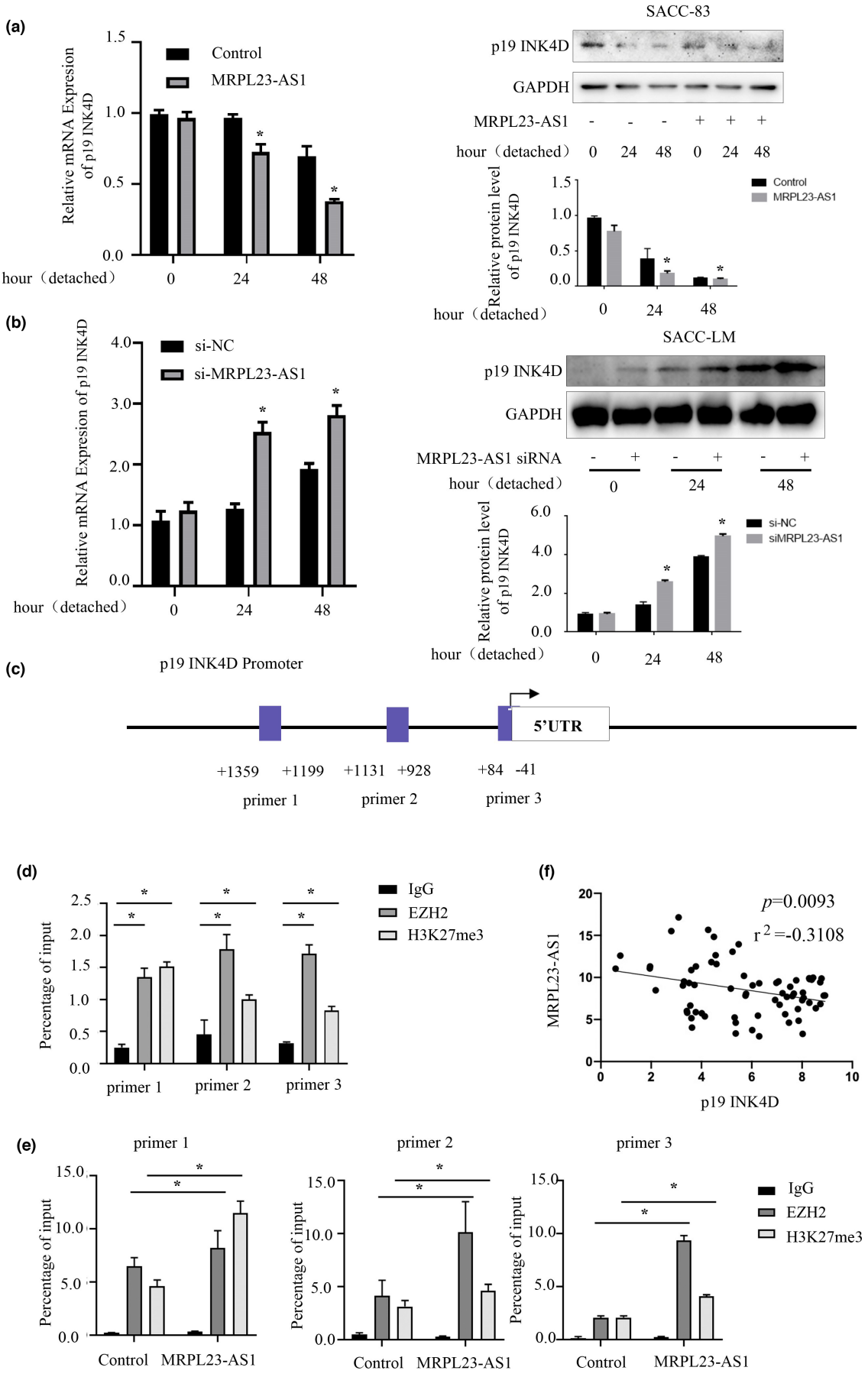

FIGURE 2 Figure Legent on next page

FIGURE 2 p19INK4D expression is involved in lncRNA MRPL23-AS1-induced anoikis resistance. (a) MRPL23-AS1 was overexpressed in SACC-83 cells. After 24 and 48 h of suspension culture, RT-PCR (left) and Western blotting (right) were used to detect changes in p19INK4D mRNA and protein. (b) MRPL23-AS1 was knocked down in SACC-LM cells, and changes in p19INK4D mRNA and protein expression were detected by RT-PCR (left) and Western blotting (right) after suspension culture for 24 and 48 hours. (c) Schematic diagram of the promoter region of p19INK4D. Black band: p19INK4D promoter region; white rectangle: 5'-UTR; blue rectangle: primer fragment designed for the predicted promoter binding site. The number indicates the number of bases from the starting base of the 5'-UTR. (d) ChIP-qPCR detected the binding of EZH2 to the promoter region of p19INK4D and the methylation status of H3K27 in the promoter region of p19INK4D in SACC-83 cells. (e) In SACC-83 cells, MRPL23-AS1 was overexpressed, and the cells were cultured in suspension for 24 h. ChIP-qPCR was used to detect the EZH2 binding and histone methylation status of the promoter region of p19INK4D. (f) The correlation between MRPL23-AS1 and p19INK4D mRNA in 106 SACC tissues was detected by RT-qPCR (r^2=-0.3108, ***p***=0.0093). The data are expressed as the mean ±SD, *p<0.05

p19INK4D and MRPL23-AS1 expression was found in SACC tissues (Figure 2f).

3.3 | P19INK4D prevents anoikis in SACC cells in vitro

To investigate whether MRPL23-AS1 prevents anoikis resistance by downregulating p19INK4D, the function of p19INK4D was evaluated in SACC cells. Western blotting and RT-PCR results indicated that the protein and mRNA expression levels of p19INK4D were significantly increased in p19INK4D overexpression vector-transfected SACC-LM cells (Figure 3a). The effects of p19INK4D on the anoikis of SACC cells were assessed using a calcein AM/PI costaining assay, and the results showed that the overexpression of p19INK4D significantly increased the percentage of dead SACC-LM cells at 12 h and 24 h after suspension culture (Figure 3b,c). Subsequently, the function of p19INK4D in SACC anoikis resistance was further investigated, and the flow cytometry results demonstrated that compared with the control conditions, p19INK4D overexpression and suspension culture for 12 h and 24 h significantly inhibited the actions of anoikis in SACC-LM cells (Figure 3d). Furthermore, Western blotting results indicated that p19INK4D overexpression increased the expression levels of the apoptosis marker activated caspase-3 but decreased the ratio of Bcl-2/bax after suspension culture for 12 and 24 h (Figure 3e). In addition, p19INK4D expression was downregulated in SACC-83 cells transfected with two p19INK4D siRNAs. Western blotting and RT-PCR results showed that p19INK4D protein and mRNA expression levels were significantly decreased in p19INK4D siRNA-transfected SACC-83 cells (Figure 3f). Moreover, we found that compared with the control conditions, p19INK4D knockdown promoted SACC-83 cell resistance to anoikis according to calcein AM/PI costaining assays and flow cytometry assays at 12 h and 24 h (Figure 3g–i). When p19INK4D was knocked down, there was a significant decrease in activated caspase-3 but a significant increase in the ratio of Bcl-2/bax (Figure 3j). These data suggest that p19INK4D promotes anoikis in SACC cells.

3.4 | *MRPL23-AS1-induced anoikis resistance in SACC cells is rescued by p19INK4D overexpression*

To further verify whether the pro-anoikis resistance effects of MRPL23-AS1 on SACC cells are mediated by the suppression of p19INK4D expression, the cell phenotype was examined after overexpressing p19INK4D in MRPL23-AS1 overexpression vector-transfected SACC-83 cells and suspension culture for 24 h. The calcein AM/PI costaining assay results suggested that p19INK4D overexpression significantly increased the percentage of dead SACC cells in the MRPL23-AS1-overexpression vector group compared with the MRPL23-AS1 vector+GV492 group (Figure 4a,b). Furthermore, the flow cytometry assay demonstrated an inhibitory effect in MRPL23-AS1-overexpressing SACC cells that overexpressed p19INK4D compared with those that expressed the MRPL23-AS1 vector+GV492 (Figure 4c). The Western blotting results suggested that overexpressing p19INK4D rescued the anoikis resistance effect of MRPL23-AS1 overexpression, as indicated by the increased expression of apoptosis marker active caspase-3 and the decreased ratio of Bcl-2/bax in MRPL23-AS1-overexpressing cells (Figure 4d,e). These findings further indicated that the overexpression of MRPL23-AS1 promotes SACC cell anoikis resistance by inhibiting the expression of p19INK4D.

3.5 | P19INK4D is downregulated in SACC and correlates with lung metastasis

We observed p19INK4D expression in 59 SACC tissue samples and 17 submandibular gland (SMG) tissue samples via IHC assay (Figure 5a and Table 1). The positive expression rate of p19INK4D in tumor tissues was significantly lower than that in SMG tissues. The difference was significant ($p < 0.05$) (Table 1). This finding was validated via analysis of the mRNA expression of p19INK4D in 106 frozen SACC tissue samples and 26 SMG tissue samples (Figure 5b). The association between clinicopathological variables and p19INK4D mRNA expression was examined in patients with SACC, and the results are presented in Table 2. All patients with SACC were classified into high-p19INK4D and low-p19INK4D groups depending on the median p19INK4D mRNA expression. Low p19INK4D mRNA expression was associated with a high incidence of lung metastasis ($p < 0.05$) (Table 2). However, no significant associations between p19INK4D mRNA expression and other clinicopathological features were observed.

4 | DISCUSSION

Lung metastasis is one of the hallmarks of SACC (Yao et al., 2018). In a previous study, we explored the role and related mechanisms of lncRNA MRPL23-AS1 in the invasion and metastasis of SACC cells

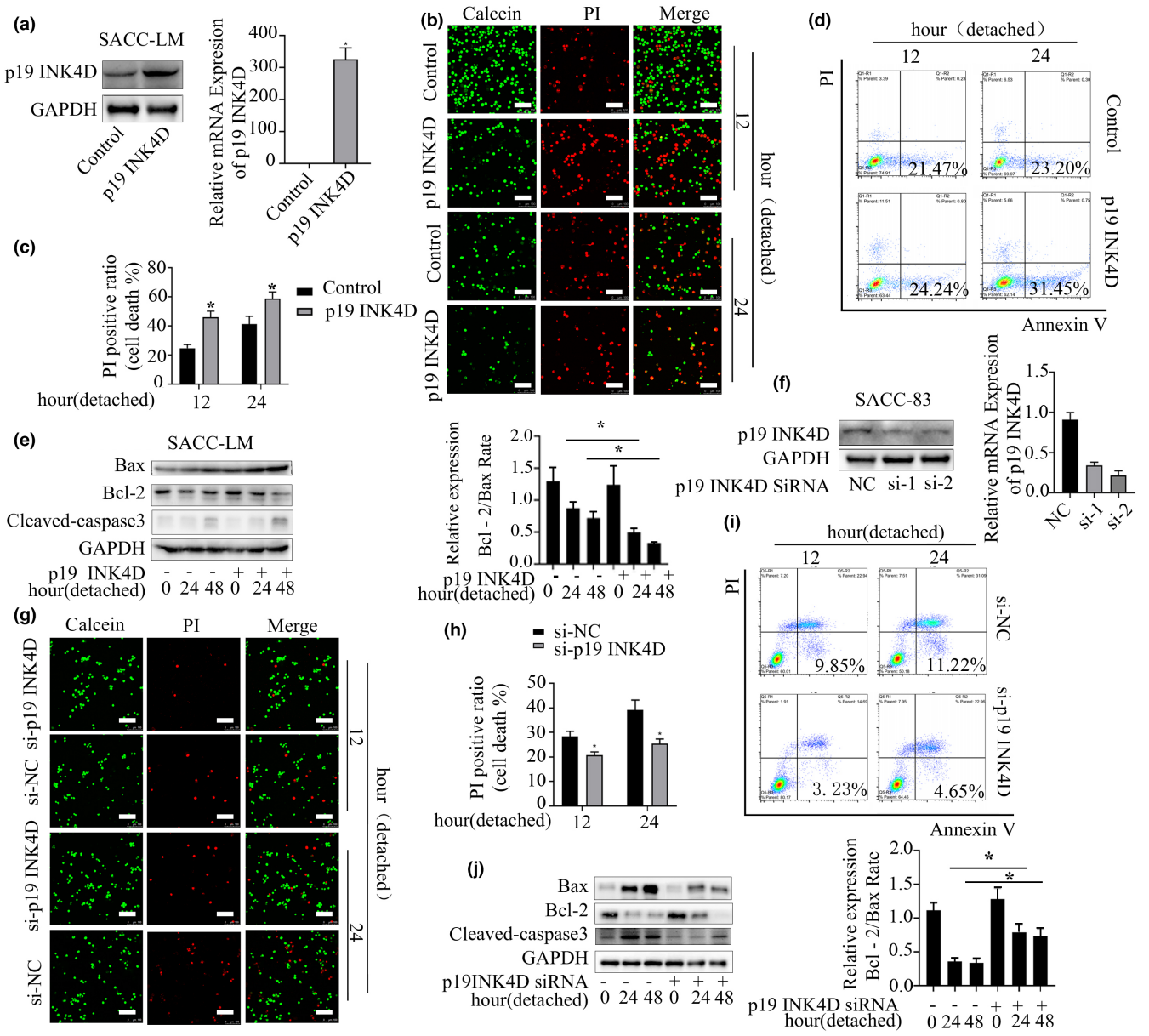

FIGURE 3 P19INK4D prevents the anoikis of SACC cells in vitro. (a) After the overexpression of p19INK4D in SACC-LM cells, the protein and mRNA expression levels were measured by Western blot (left) and RT-PCR (right), respectively, to assess efficiency. (b, c) After the overexpression of p19INK4D and 12 and 24 h of suspension culture, SACC-LM cells were stained with calcein AM/PI. Five fields of view were chosen, and the cell death rate was determined. Scale bar =100 μm. (d) The percentage of apoptotic cells was determined by flow cytometry with annexin V-FITC-PI staining of in SACC-LM cells with overexpression of p19INK4D, followed by suspension culture for 12 and 24 h. FITC: fluorescein isothiocyanate; PI: propidium iodide. (e) Overexpression of p19INK4D in SACC-LM cells followed by suspension culture for 24 and 48 hours. Apoptosis-related proteins were detected by Western blotting (left). The relative expression of Bcl-2-Bax was determined by Western blot analysis (right). (f) The knockdown efficiency of p19INK4D siRNA was measured by Western blotting and qRT-PCR in SACC-83 cells. (g-h) After knockdown of p19INK4D in SACC-83 cells and suspension culture for 12 and 24 hours, the cells were stained with calcein AM and PI. Five fields were chosen for each group, and the cell death rate was determined. Scale bar= 100 μm. (i) After knockdown of p19INK4D in SACC-83 cells and suspension culture for 12 and 24 h, the percentage of apoptotic cells was determined by flow cytometry with annexin V-FITC/PI staining. FITC: fluorescein isothiocyanate; PI: propidium iodide. (j) p19INK4D was knocked down in SACC-83 cells, and apoptosis-related proteins were measured by Western blot after suspension culture for 24 and 48 h (left). The relative expression of Bcl-2-Bax determined by Western blot analysis (right) (*$p < 0.05$; the data are expressed as the mean ± SD; $n = 3$)

(Chen et al., 2020). The study revealed that MRPL23-AS1 contributes to SACC cell invasion and metastasis by recruiting EZH2 and thus negatively regulates the expression of E-cadherin (Chen et al., 2020). The mechanism of metastasis is closely related to anoikis sensitivity. Anoikis is a type of apoptosis that occurs in the process of metastasis after cells enter the blood vessel (Komata et al., 2003; Zhang et al., 2009). The ability of tumor cells to resist anoikis that occurs after cells break away from the extracellular matrix is essential

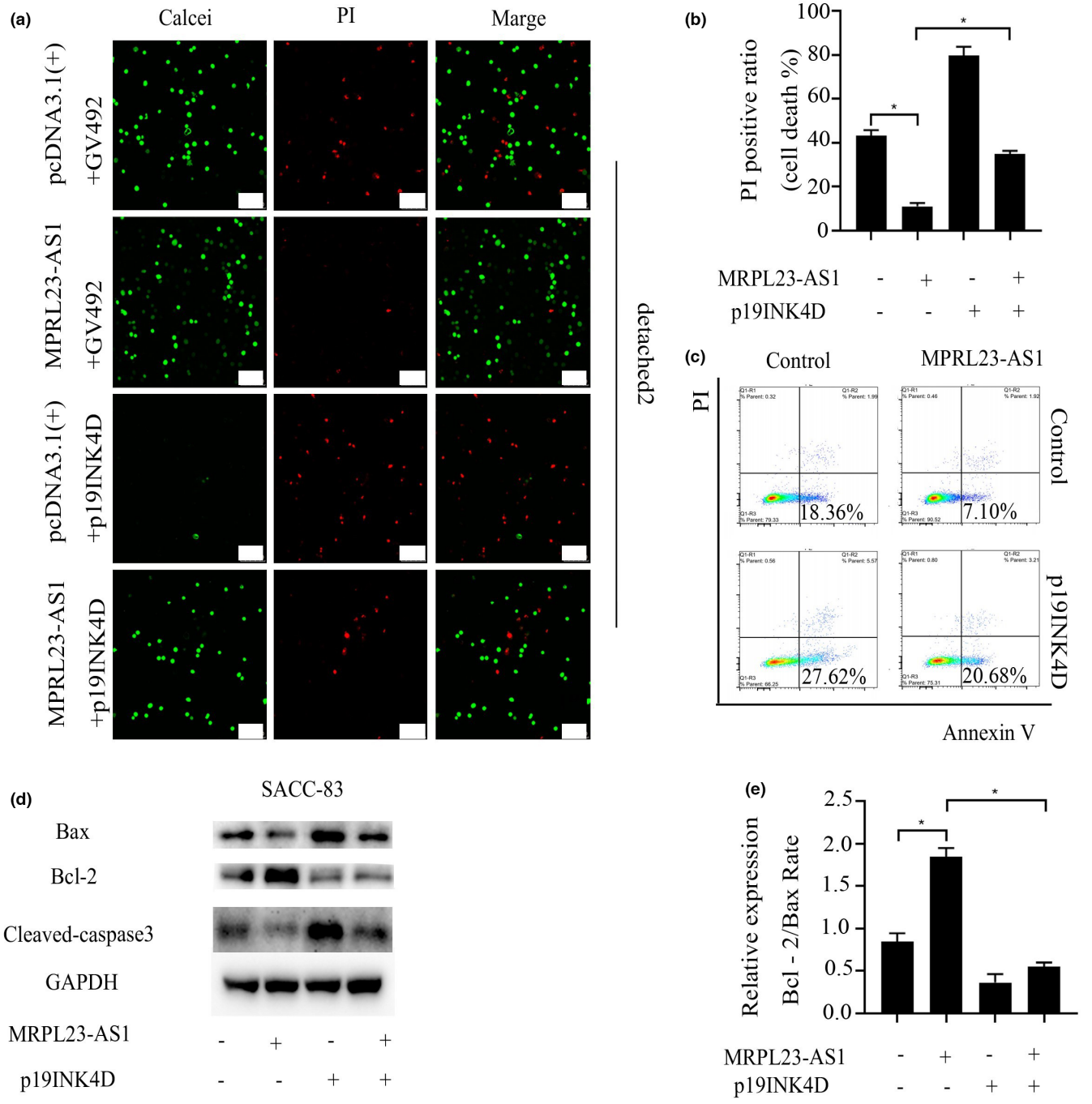

FIGURE 4 MRPL23-AS1-induced anoikis resistance in SACC cells is rescued by p19INK4D overexpression. (a, b) MRPL23-AS1 and p19INK4D overexpression vectors and their controls (pcDNA3.1(+) and GV492, respectively) were transfected into SACC-83 cells, which were cultured in suspension for 24 h and then stained with calcein AM/PI. Five fields were chosen for each group, and the cell death rate was determined. Scale bar= 20 μm. (c) After transfection of MRPL23-AS1 and p19INK4D and their control vectors in SACC-83 cells and suspension culture of the cells for 24 h, the percentage of apoptotic cells was determined by flow cytometry with annexin V-FITC/PI staining. FITC: fluorescein isothiocyanate; PI: propidium iodide. (d) SACC-83 cells overexpressing MRPL23-AS1 and p19INK4D and their control vectors were cultured in suspension for 24 h. Western blotting was performed to detect the expression of apoptosis-related proteins. (e) The Bcl-2/Bax ratio was determined by Western blotting with semiquantitative analysis (*$p < 0.05$; the data are expressed as the mean ± SD; $n = 3$)

for the successful metastasis of tumor cells to distant target organs, including the lung. Previous studies have also reported that certain lncRNAs promote anoikis resistance: The lncRNA MALAT1 facilitates a pro-metastatic phenotype by altering the expression of anoikis resistance-related genes in ovarian cancer (Gordon et al., 2019), and the lncRNA HOTAIR regulates the anoikis resistance capacity and spheroid formation of ovarian cancer cells (Dai et al., 2021). The function and molecular mechanism of MRPL23-AS1 in

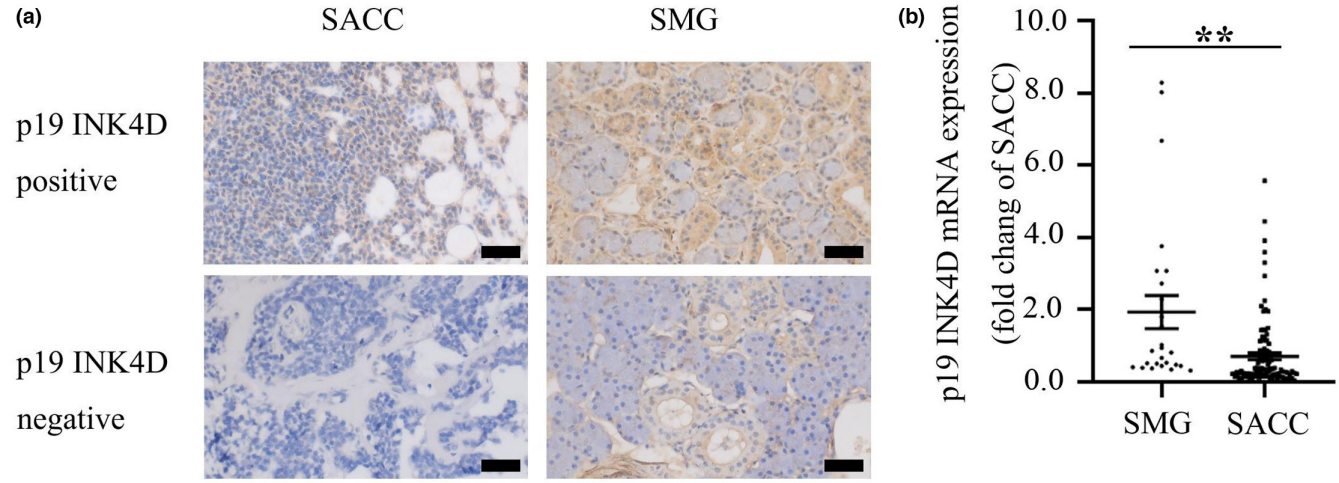

FIGURE 5 P19INK4D expression in human tissues. (a) Immunohistochemical analysis of P19INK4D expression in human SACC tissue samples and normal SMG tissue samples. Scale bar = 50 μm. (b) Real-time PCR analysis of p19INK4D mRNA expression in 106 human SACC tissue samples and 26 normal SMG tissue samples. *$p < 0.05$, Mann–Whitney U rank sum test

TABLE 1 Immunohistochemical analysis of p19INK4D protein levels in 59 SACC tumors and 17 normal submandibular gland (SMG) tissues

IHC	p19INK4D expression in tumor tissues		
Tissue	Positive	Negative	Total
SMG	17 (100%)	0 (0%)	17
SACC	33 (55.93%)	26 (44.07%)	59
Total	50	26	76
$\chi 2$	11.39		
p-value	0.0007		

SACC anoikis resistance remain unknown. The present results suggest that the overexpression of MRPL23-AS1 promoted anoikis resistance in SACC-83 cells, while MRPL23-AS1 knockdown inhibited anoikis resistance in highly metastatic SACC-LM cells by calcein AM/PI costaining assay and flow cytometry assay. Further examination by Western blotting revealed that MRPL23-AS1 overexpression downregulated apoptosis markers and vice versa. These data underline a novel role of MRPL23-AS1 in anoikis resistance, a feature of tumors in the metastasis process. Its regulatory effects on the anoikis of SACC cells suggested that MRPL23-AS1-induced anoikis resistance is a unknown mechanism that increases tumor malignancy.

A previous study indicated that MRPL23-AS1 inhibits downstream gene expression by recruiting EZH2 to the downstream molecular promoter region and regulates SACC tumor cell EMT to promote lung metastasis (Chen et al., 2020). To identify the downstream target gene in the process of anoikis resistance, we evaluated the expression of several potential downstream genes that are regulated by the silencing of EZH2 (Ferraro et al., 2013; Joyce et al., 2009). After changing MRPL23-AS1 expression and suspension culture, we found that p19INK4D expression negatively correlated with MRPL23-AS1 expression by Western blotting and RT-PCT assay. However, after altering MRPL23-AS1 expression in SACC cells, there was no change in p19INK4D expression upon adherent culture. p19INK4D, a member of the INK4 family, leads cells to arrest in the G1 phase by competitively binding cyclin D-CDK4/6 and inhibiting the formation of the corresponding complex (Cheng, 2004). A previous study showed that p19INK4D expression is associated with sensitization to cell death after drug-induced DNA damage in MYCN-amplified neuroblastoma cells (Gogolin et al., 2013). p19INK4D also mediates apoptosis by activating caspases in MDA-MB-231 cells (Guo et al., 2013), and p19INK4D blocks the cell cycle to induce the apoptosis of hepatocellular carcinoma cells (Zhou et al., 2018) and has an antitumor effect against malignant glioma cells (Komata et al., 2003). The upregulation of p19INK4D can promote apoptosis by activating the caspase pathway (Guo et al., 2013); however, the role of p19INK4D in anoikis is unclear. Therefore, p19INK4D may act downstream of MRPL23-AS1 and participate in the regulation of anoikis in tumor cells. MRPL23-AS1 promotes the binding of EZH2 and the E-cad promoter region to downregulate the expression of E-cad and promote tumor metastasis in SACC (Chen et al., 2020). However, whether the EZH2 and p19INK4D promoters combine has not yet been reported. To further clarify the relationship between MRPL23-AS1 and p19INK4D in SACC cells, a ChIP assay was used to verify the EZH2 binding sites on the p19INK4D promoter predicted by the website. There were three potential binding sites for EZH2 on the p19INK4D promoter, and after the overexpression of MRPL23-AS1 followed by suspension culture, the intensity of the band of the promoter and EZH2 increased. It was further found by RT-PCR that in SACC tissues, the expression levels of MRPL23-AS1 and p19INK4D were negatively correlated. These results show that p19INK4D is transcriptionally silenced by MRPL23-AS1 via EZH2-mediated H3K27me3 modification and is involved in anoikis resistance in SACC. Knockdown of p19INK4D promoted SACC cell resistance to anoikis and apoptosis markers downregulation, whereas p19INK4D overexpression had the opposite effect.

TABLE 2 Correlation between clinicopathological variables and p19INK4D expression in patients with SACC

Variables	p19INK4D expression			$\chi 2$	*p*-value
	Total (*n*)	Low (*n*)	High (*n*)		
Age, years				0.01196	0.9129
<42	27	13	14		
≥42	79	39	40		
Sex				0.316	0.574
Male	46	24	22		
Female	60	28	32		
Tumor size				0.5861	0.4439
<4 cm	75	35	40		
≥4 cm	31	17	14		
Clinical stage				3.775	0.052
I/II	53	21	32		
III/IV	53	31	22		
Lymph node metastasis				0.1662	0.6835
Absent	97	47	50		
Present	9	5	4		
Perineural invasion				1.002	0.3167
Absent	79	41	38		
Present	27	11	16		
Lung metastasis				4.23	0.0397
Absent	96	44	52		
Present	10	8	2		
Local regional recurrence				0.5975	0.4395
Absent	77	36	41		
Present	29	16	13		
Pathological type				0.3242	0.5691
Cribriform/ Tubular	82	39	43		
Solid	24	13	11		

In this study, p19INK4D expression was lower in SACC tissues than in SMG tissues. In addition, we first showed the negative relationship between p19INK4D expression and metastasis to the lung, which significantly correlated with a poor prognosis in SACC patients. Low tissue levels of p19INK4D in tumors are a predictor of poor prognosis in patients with hepatocellular carcinoma (Zhou et al., 2018). Collectively, these results suggest that p19INK4D may be a tumor suppressor gene in SACC and may promote tumor cell anoikis.

The present study focused on the effects of MRPL23-AS1 on anoikis resistance in SACC cells. MRPL23-AS1 may also be involved in other tumor processes, and the exact binding sequence of the p19INK4D promoter bound by EZH2 is unknown. Future investigations should focus on verifying this mechanism in vivo and determining whether the MRPL23-AS1/p19INK4D axis can lead to clinical antitumor treatment. In addition, lncRNAs regulate the expression of genes, acting in the form of cis in the nucleus, or of genes in other parts of the cell, acting in the form of trans in the nucleus or cytoplasm, by interacting with proteins, RNA and DNA. LncRNAs can positively or negatively regulate gene expression through a variety of mechanisms, including the recruitment of transcription factors or chromatin modification complexes to specific gene sites to form a heterogeneous ribonucleoprotein complex (hnRNP) to isolate RNA binding proteins (RBPs) and microRNAs or through directly binding to RNA and DNA through base complementary pairing (Guttman & Rinn, 2012; Quinn & Chang, 2016; Rinn & Chang, 2012). First, one of the most important functions of lncRNAs is to inhibit or activate chromatin through cis (Wang et al., 2008). Second, HOX antisense intergenic RNA (HOTAIR) is one of the first reported lncRNAs that regulate gene expression through a trans-acting mode. During development, HOTAIR inhibits transcription by recruiting the PRC2 protein to play a trans role at the HOX D site (Rinn et al., 2007; Tsai et al., 2010). The third type of lncRNA is exported to the cytoplasm to perform its regulatory role (Lin et al., 2016). A previous study has shown that MRPL23-AS1 localizes to the nucleus (Chen et al., 2020); thus, we consider it more likely that MRPL23-AS1 binds to protein, DNA, or RNA in the nucleus than to miRNA in the cytoplasm. CHIRP results showed that MRPL23-AS1 binds to the promoter region DNA of EZH2 and E-cadherin (Chen et al., 2020). Based on these research foundations, we conducted a more complete study on the function of MRPL23-AS1 in the nucleus; however, whether it has other biological functions as a lncRNA in the cell remains to be further studied.

In conclusion, the present results demonstrate that MRPL23-AS1 acts as an oncogene in SACC by facilitating resistance to tumor cell anoikis, which is promoted by the EZH2-mediated hypermethylation of histones in the promoter region of p19INK4D. The identification of the novel MRPL23-AS1/p19INK4D axis is significant for understanding the mechanisms of SACC metastasis and offers further insights into the identification of novel biomarkers or potential therapeutic targets for SACC.

ACKNOWLEDGMENTS

This study was supported by Beijing Natural Science Foundation (grant no. 7222225) and National Natural Science Foundation of China (grant no. 82173307 and no. 81872190).

CONFLICTS OF INTEREST

None to declare.

AUTHOR CONTRIBUTIONS

Min Fu: Data curation; Methodology; Project administration; Visualization. **Ye-Qing Song:** Data curation; Methodology; Software. **Sheng-lin Li:** Methodology; Supervision; Visualization. **Xi-Yuan Ge:** Resources; Supervision; Writing – review & editing.

DATA AVAILABILITY STATEMENT

The datasets used and/or analyzed in the current study are available from the corresponding author upon reasonable request.

ORCID

Yin-Ran Li https://orcid.org/0000-0002-8143-6257

REFERENCES

Besson, A., Dowdy, S. F., & Roberts, J. M. (2008). CDK inhibitors: Cell cycle regulators and beyond. *Developmental Cell*, *14*(2), 159–169. https://doi.org/10.1016/j.devcel.2008.01.013

Carcagno, A. L., Giono, L. E., Marazita, M. C., Castillo, D. S., Pregi, N., & Cánepa, E. T. (2012). E2F1 induces p19INK4d, a protein involved in the DNA damage response, following UV irradiation. *Molecular and Cellular Biochemistry*, *366*(1–2), 123–129. https://doi.org/10.1007/s11010-012-1289-8

Chen, C. W., Fu, M., Du, Z. H., Zhao, F., Yang, W. W., Xu, L. H., & Ge, X. Y. (2020). Long noncoding RNA MRPL23-AS1 promoteoid cystic carcinoma lung metastasis. *Cancer Research*, *80*, 2273–2285. https://doi.org/10.1158/0008-5472.Can-19-0819

Chen, W., Dong, S., Zhou, J., & Sun, M. (2012). Investigation of myoepithelial cell differentiation into Schwann-like cells in salivary adenoid cystic carcinoma associated with perineural invasion. *Molecular Medicine Reports*, *6*, 755–759. https://doi.org/10.3892/mmr.2012.1003

Cheng, T. (2004). Cell cycle inhibitors in normal and tumor stem cells. *Oncogene*, *23*, 7256–7266. https://doi.org/10.1038/sj.onc.1207945

Coca-Pelaz, A., Rodrigo, J. P., Bradley, P. J., Vander Poorten, V., Triantafyllou, A., Hunt, J. L., Strojan, P., Rinaldo, A., Haigentz, M., Takes, R. P., Mondin, V., Teymoortash, A., Thompson, L. D. R., & Ferlito, A. (2015). Adenoid cystic carcinoma of the head and neck–An update. *Oral Oncology*, *51*, 652–661. https://doi.org/10.1016/j.oraloncology.2015.04.005

Dai, Z. Y., Jin, S. M., Luo, H. Q., Leng, H. L., & Fang, J. D. (2021). LncRNA HOTAIR regulates anoikis-resistance capacity and spheroid formation of ovarian cancer cells by recruiting EZH2 and influencing H3K27 methylation. *Neoplasma*, *68*(03), 509–518. https://doi.org/10.4149/neo_2021_201112N1212

Diao, B., Liu, Y., Xu, G. Z., Zhang, Y., Xie, J., & Gong, J. (2018). The role of galectin-3 in the tumorigenesis and progression of pituitary tumors. *Oncology Letters*, *15*, 4919–4925. https://doi.org/10.3892/ol.2018.7931

Dong, L., Wang, Y. X., Li, S. L., Yu, G. Y., Gan, Y. H., Li, D., & Wang, C. Y. (2011). TGF-beta1 promotes migration and invasion of salivary adenoid cystic carcinoma. *Journal of Dental Research*, *90*(6), 804–809. https://doi.org/10.1177/0022034511401407

Dreidax, D., Bannert, S., Henrich, K.-O., Schröder, C., Bender, S., Oakes, C. C., Lindner, S., Schulte, J. H., Duffy, D., Schwarzl, T., Saadati, M., Ehemann, V., Benner, A., Pfister, S., Fischer, M., & Westermann, F. (2014). p19-INK4d inhibits neuroblastoma cell growth, induces differentiation and is hypermethylated and downregulated in MYCN-amplified neuroblastomas. *Human Molecular Genetics*, *23*, 6826–6837. https://doi.org/10.1093/hmg/ddu406

Ellington, C. L., Goodman, M., Kono, S. A., Grist, W., Wadsworth, T., Chen, A. Y., Owonikoko, T., Ramalingam, S., Shin, D. M., Khuri, F. R., Beitler, J. J., & Saba, N. F. (2012). Adenoid cystic carcinoma of the head and neck: Incidence and survival trends based on 1973–2007 Surveillance, Epidemiology, and End Results data. *Cancer*, *118*(18), 4444–4451. https://doi.org/10.1002/cncr.27408

Ferraro, A., Mourtzoukou, D., Kosmidou, V., Avlonitis, S., Kontogeorgos, G., Zografos, G., & Pintzas, A. (2013). EZH2 is regulated by ERK/AKT and targets integrin alpha2 gene to control Epithelial-Mesenchymal Transition and anoikis in colon cancer cells. *International Journal of Biochemistry & Cell Biology*, *45*(2), 243–254. https://doi.org/10.1016/j.biocel.2012.10.009

Fu, M., Chen, C. W., Yang, L. Q., Yang, W. W., Du, Z. H., Li, Y. R., Li, S. L., & Ge, X. Y. (2020). MicroRNA-103a-3p promotes metastasis by targeting TPD52 in salivary adenoid cystic carcinoma. *International Journal of Oncology*, *57*(2), 574–586. https://doi.org/10.3892/ijo.2020.5069

Gao, M., Hao, Y., Huang, M. X., Ma, D. Q., Luo, H. Y., Gao, Y., Peng, X., & Yu, G. Y. (2013). Clinicopathological study of distant metastases of salivary adenoid cystic carcinoma. *International Journal of Oral and Maxillofacial Surgery*, *42*, 923–928. https://doi.org/10.1016/j.ijom.2013.04.006

Gilles, L., Guièze, R., Bluteau, D., Cordette-Lagarde, V., Lacout, C., Favier, R., Larbret, F., Debili, N., Vainchenker, W., & Raslova, H. (2008). P19INK4D links endomitotic arrest and megakaryocyte maturation and is regulated by AML-1. *Blood*, *111*, 4081–4091. https://doi.org/10.1182/blood-2007-09-113266

Gillies, R. J., Robey, I., & Gatenby, R. A. (2008). Causes and consequences of increased glucose metabolism of cancers. *Journal of Nuclear Medicine*, *49*(Suppl 2), 24s–42s. https://doi.org/10.2967/jnumed.107.047258

Gogolin, S., Ehemann, V., Becker, G., Brueckner, L. M., Dreidax, D., Bannert, S., & Westermann, F. (2013). CDK4 inhibition restores G(1)-S arrest in MYCN-amplified neuroblastoma cells in the context of doxorubicin-induced DNA damage. *Cell Cycle*, *12*, 1091–1104. https://doi.org/10.4161/cc.24091

Gordon, M. A., Babbs, B., Cochrane, D. R., Bitler, B. G., & Richer, J. K. (2019). The long non-coding RNA MALAT1 promotes ovarian cancer progression by regulating RBFOX2-mediated alternative splicing. *Molecular Carcinogenesis*, *58*(2), 196–205. https://doi.org/10.1002/mc.22919

Guo, M., Wang, M., Deng, H., Zhang, X., & Wang, Z. Y. (2013). A novel anticancer agent Broussoflavonol B downregulates estrogen receptor (ER)-α36 expression and inhibits growth of ER-negative breast cancer MDA-MB-231 cells. *European Journal of Pharmacology*, *714*(1–3), 56–64. https://doi.org/10.1016/j.ejphar.2013.05.047

Guttman, M., & Rinn, J. L. (2012). Modular regulatory principles of large non-coding RNAs. *Nature*, *482*(7385), 339–346. https://doi.org/10.1038/nature10887

Hilpert, M., Legrand, C., Bluteau, D., Balayn, N., Betems, A., Bluteau, O., Villeval, J.-L., Louache, F., Gonin, P., Debili, N., Plo, I., Vainchenker, W., Gilles, L., & Raslova, H. (2014). p19 INK4d controls hematopoietic stem cells in a cell-autonomous manner during genotoxic stress and through the microenvironment during aging. *Stem Cell Reports*, *3*, 1085–1102. https://doi.org/10.1016/j.stemcr.2014.10.005

Hu, H., Miao, Y. R., Jia, L. H., Yu, Q. Y., Zhang, Q., & Guo, A. Y. (2019). AnimalTFDB 3.0: A comprehensive resource for annotation and prediction of animal transcription factors. *Nucleic Acids Research*, *47*(D1), D33–D38. https://doi.org/10.1093/nar/gky822

Ivanchuk, S. M., Mondal, S., Dirks, P. B., & Rutka, J. T. (2001). The INK4A/ARF locus: Role in cell cycle control and apoptosis and implications for glioma growth. *Journal of Neuro-Oncology*, *51*, 219–229. https://doi.org/10.1023/a:1010632309113

Joyce, T., Cantarella, D., Isella, C., Medico, E., & Pintzas, A. (2009). A molecular signature for Epithelial to Mesenchymal transition in a human colon cancer cell system is revealed by large-scale microarray analysis. *Clinical & Experimental Metastasis*, *26*(6), 569–587. https://doi.org/10.1007/s10585-009-9256-9

Kapranov, P., Cheng, J., Dike, S., Nix, D. A., Duttagupta, R., Willingham, A. T., Stadler, P. F., Hertel, J., Hackermüller, Jörg, Hofacker, I. L., Bell, I., Cheung, E., Drenkow, J., Dumais, E., Patel, S., Helt, G., Ganesh, M., Ghosh, S., Piccolboni, A., … Gingeras, T. R. (2007). RNA maps reveal new RNA classes and a possible function for pervasive transcription. *Science*, *316*, 1484–1488. https://doi.org/10.1126/science.1138341

Kokemueller, H., Eckardt, A., Brachvogel, P., & Hausamen, J. E. (2004). Adenoid cystic carcinoma of the head and neck–a 20 years experience. *International Journal of Oral and Maxillofacial Surgery*, *33*(1), 25–31.

Komata, T., Kanzawa, T., Takeuchi, H., Germano, I. M., Schreiber, M., Kondo, Y., & Kondo, S. (2003). Antitumour effect of cyclin-dependent kinase inhibitors (p16(INK4A), p18(INK4C), p19(INK4D), p21(WAF1/CIP1) and p27(KIP1)) on malignant glioma cells. *British Journal of Cancer*, *88*, 1277–1280. https://doi.org/10.1038/sj.bjc.6600862

Kong, J., Tian, H., Zhang, F., Zhang, Z., Li, J., Liu, X., Li, X., Liu, J., Li, X., Jin, D., Yang, X., Sun, B. O., Guo, T., Luo, Y., Lu, Y., Lin, B., & Liu, T. (2019). Extracellular vesicles of carcinoma-associated fibroblasts creates a pre-metastatic niche in the lung through activating fibroblasts. *Molecular Cancer*, *18*(1), 175. https://doi.org/10.1186/s12943-019-1101-4

Li, S. L. (1990). Establishment of a human cancer cell line from adenoid cystic carcinoma of the minor salivary gland. *Zhonghua Kou Qiang Yi Xue Za Zhi*, *25*(1), 29–31, 62.

Lin, A., Li, C., Xing, Z., Hu, Q., Liang, K. E., Han, L., Wang, C., Hawke, D. H., Wang, S., Zhang, Y., Wei, Y., Ma, G., Park, P. K., Zhou, J., Zhou, Y., Hu, Z., Zhou, Y., Marks, J. R., Liang, H., … Yang, L. (2016). The LINK-A lncRNA activates normoxic HIF1α signalling in triple-negative breast cancer. *Nature Cell Biology*, *18*(2), 213–224. https://doi.org/10.1038/ncb3295

Liu, X., Fu, Q., Bian, X., Fu, Y., Xin, J., Liang, N., Li, S., Zhao, Y., Fang, L. I., Li, C., Zhang, J., Dionigi, G., & Sun, H. (2020). Long non-coding RNA MAPK8IP1P2 inhibits lymphatic metastasis of thyroid cancer by activating hippo signaling via sponging miR-146b-3p. *Frontiers in Oncology*, *10*, 600927. https://doi.org/10.3389/fonc.2020.600927

Lloyd, S., Yu, J. B., Wilson, L. D., & Decker, R. H. (2011). Determinants and patterns of survival in adenoid cystic carcinoma of the head and neck, including an analysis of adjuvant radiation therapy. *American Journal of Clinical Oncology*, *34*(1), 76–81. https://doi.org/10.1097/COC.0b013e3181d26d45

Martinou, J. C., & Youle, R. J. (2011). Mitochondria in apoptosis: Bcl-2 family members and mitochondrial dynamics. *Developmental Cell*, *21*(1), 92–101. https://doi.org/10.1016/j.devcel.2011.06.017

Medema, J. P., Scaffidi, C., Kischkel, F. C., Shevchenko, A., Mann, M., Krammer, P. H., & Peter, M. E. (1997). FLICE is activated by association with the CD95 death-inducing signaling complex (DISC). *EMBO Journal*, *16*, 2794–2804. https://doi.org/10.1093/emboj/16.10.2794

Quinn, J. J., & Chang, H. Y. (2016). Unique features of long non-coding RNA biogenesis and function. *Nature Reviews Genetics*, *17*(1), 47–62. https://doi.org/10.1038/nrg.2015.10

Rapidis, A. D., Givalos, N., Gakiopoulou, H., Faratzis, G., Stavrianos, S. D., Vilos, G. A., Douzinas, E. E., & Patsouris, E. (2005). Adenoid cystic carcinoma of the head and neck. Clinicopathological analysis of 23 patients and review of the literature. *Oral Oncology*, *41*, 328–335. https://doi.org/10.1016/j.oraloncology.2004.12.004

Rinn, J. L., & Chang, H. Y. (2012). Genome regulation by long noncoding RNAs. *Annual Review of Biochemistry*, *81*, 145–166. https://doi.org/10.1146/annurev-biochem-051410-092902

Rinn, J. L., Kertesz, M., Wang, J. K., Squazzo, S. L., Xu, X., Brugmann, S. A., Goodnough, L. H., Helms, J. A., Farnham, P. J., Segal, E., & Chang, H. Y. (2007). Functional demarcation of active and silent chromatin domains in human HOX loci by noncoding RNAs. *Cell*, *129*(7), 1311–1323. https://doi.org/10.1016/j.cell.2007.05.022

Roskoski, R. Jr (2019). Cyclin-dependent protein serine/threonine kinase inhibitors as anticancer drugs. *Pharmacological Research*, *139*, 471–488. https://doi.org/10.1016/j.phrs.2018.11.035

Sanchez-Ruderisch, H., Fischer, C., Detjen, K. M., Welzel, M., Wimmel, A., Manning, J. C., André, S., & Gabius, H.-J. (2010). Tumor suppressor p16 INK4a: Downregulation of galectin-3, an endogenous competitor of the pro-anoikis effector galectin-1, in a pancreatic carcinoma model. *FEBS Journal*, *277*(17), 3552–3563. https://doi.org/10.1111/j.1742-4658.2010.07764.x

Sonzogni, S. V., Ogara, M. F., Belluscio, L. M., Castillo, D. S., Scassa, M. E., & Cánepa, E. T. (2014). p19INK4d is involved in the cellular senescence mechanism contributing to heterochromatin formation. *Biochimica Et Biophysica Acta*, *1840*(7), 2171–2183. https://doi.org/10.1016/j.bbagen.2014.03.015

Spiro, R. H. (1997). Distant metastasis in adenoid cystic carcinoma of salivary origin. *American Journal of Surgery*, *174*, 495–498. https://doi.org/10.1016/s0002-9610(97)00153-0

Spiro, R. H., & Huvos, A. G. (1992). Stage means more than grade in adenoid cystic carcinoma. *American Journal of Surgery*, *164*, 623–628. https://doi.org/10.1016/s0002-9610(05)80721-4

Tajbakhsh, A., Rivandi, M., Abedini, S., Pasdar, A., & Sahebkar, A. (2019). Regulators and mechanisms of anoikis in triple-negative breast cancer (TNBC): A review. *Critical Reviews in Oncology/Hematology*, *140*, 17–27. https://doi.org/10.1016/j.critrevonc.2019.05.009

Terhaard, C. H. J., Lubsen, H., Van der Tweel, I., Hilgers, F., Eijkenboom, W., Marres, H., Tjho-Heslinga, R. E., de Jong, J., & Roodenburg, J. (2004). Salivary gland carcinoma: Independent prognostic factors for locoregional control, distant metastases, and overall survival: Results of the Dutch head and neck oncology cooperative group. *Head & Neck*, *26*, 681–692. https://doi.org/10.1002/hed.10400

Tian, H., Lian, R., Li, Y., Liu, C., Liang, S., Li, W., Tao, T., Wu, X., Ye, Y., Yang, X., Han, J., Chen, X., Li, J., He, Y., Li, M., Wu, J., & Cai, J. (2020). AKT-induced lncRNA VAL promotes EMT-independent metastasis through diminishing Trim16-dependent Vimentin degradation. *Nature Communications*, *11*, 5127. https://doi.org/10.1038/s41467-020-18929-0

Tincani, A. J., Del Negro, A., Araújo, P. P. C., Akashi, H. K., Martins, A. S., Altemani, A. M., & Barreto, G. (2006). Management of salivary gland adenoid cystic carcinoma: Institutional experience of a case series. *Sao Paulo Medical Journal*, *124*(1), 26–30. https://doi.org/10.1590/s1516-31802006000100006

Topel, H., Bagirsakci, E., Comez, D., Bagci, G., Cakan-Akdogan, G., & Atabey, N. (2020). lncRNA HOTAIR overexpression induced downregulation of c-Met signaling promotes hybrid epithelial/mesenchymal phenotype in hepatocellular carcinoma cells. *Cell Communication and Signaling*, *18*(1), 110. https://doi.org/10.1186/s12964-020-00602-0

Tsai, M.-C., Manor, O., Wan, Y., Mosammaparast, N., Wang, J. K., Lan, F., Shi, Y., Segal, E., & Chang, H. Y. (2010). Long noncoding RNA as modular scaffold of histone modification complexes. *Science*, *329*(5992), 689–693. https://doi.org/10.1126/science.1192002

van der Wal, J. E., Becking, A. G., Snow, G. B., & van der Waal, I. (2002). Distant metastases of adenoid cystic carcinoma of the salivary glands and the value of diagnostic examinations during follow-up. *Head & Neck*, *24*, 779–783. https://doi.org/10.1002/hed.10126

Wang, K. C., & Chang, H. Y. (2011). Molecular mechanisms of long noncoding RNAs. *Molecular Cell*, *43*, 904–914. https://doi.org/10.1016/j.molcel.2011.08.018

Wang, X., Arai, S., Song, X., Reichart, D., Du, K., Pascual, G., Tempst, P., Rosenfeld, M. G., Glass, C. K., & Kurokawa, R. (2008). Induced ncRNAs allosterically modify RNA-binding proteins in cis to inhibit transcription. *Nature*, *454*(7200), 126–130. https://doi.org/10.1038/nature06992

Yao, X., Wang, Y. U., Duan, Y., Zhang, Q., Li, P., Jin, R., Tao, Y., Zhang, W., Wang, X., Jing, C., & Zhou, X. (2018). IGFBP2 promotes salivary adenoid cystic carcinoma metastasis by activating the NF-κB/ZEB1 signaling pathway. *Cancer Letters*, *432*, 38–46. https://doi.org/10.1016/j.canlet.2018.06.008

Zhang, H., Liu, S., Tang, L., Ge, J., & Lu, X. (2021). Long non-coding RNA (LncRNA) MRPL23-AS1 promotes tumor progression and carcinogenesis in osteosarcoma by activating Wnt/β-catenin

signaling via inhibiting microRNA miR-30b and upregulating myosin heavy chain 9 (MYH9). *Bioengineered*, *12*(1), 162–171. https://doi.org/10.1080/21655979.2020.1863014

Zhang, S. Q., Yu, H., & Zhang, L. L. (2009). Clinical implications of increased lymph vessel density in the lymphatic metastasis of early-stage invasive cervical carcinoma: a clinical immunohistochemical method study. *BMC Cancer*, *9*, 64. https://doi.org/10.1186/1471-2407-9-64

Zhou, H., Cai, Y., Liu, D., Li, M., Sha, Y., Zhang, W., & Xia, J. (2018). Pharmacological or transcriptional inhibition of both HDAC1 and 2 leads to cell cycle blockage and apoptosis via p21(Waf1/Cip1) and p19(INK4d) upregulation in hepatocellular carcinoma. *Cell Proliferation*, *51*(3), e12447. https://doi.org/10.1111/cpr.12447

SUPPORTING INFORMATION

Additional supporting information may be found in the online version of the article at the publisher's website.

How to cite this article: Li, Y.-R., Fu, M., Song, Y.-Q., Li, S.-L., & Ge, X.-Y. (2023). Long non-coding RNA MRPL23-AS1 suppresses anoikis in salivary adenoid cystic carcinoma in vitro. *Oral Diseases*, *29*, 1588–1601. https://doi.org/10.1111/odi.14156